Predictability of Mediterranean climate variables from oceanic variability - part II: statistical models for monthly precipitation and temperature in the Mediterranean area

Elke Hertig, Jucundus Jacobeit

Angaben zur Veröffentlichung / Publication details:

Hertig, Elke, and Jucundus Jacobeit. 2011. "Predictability of Mediterranean climate variables from oceanic variability - part II: statistical models for monthly precipitation and temperature in the Mediterranean area." *Climate Dynamics* 36 (5-6): 825–43. https://doi.org/10.1007/s00382-010-0821-3.

Predictability of Mediterranean climate variables from oceanic variability. Part II: Statistical models for monthly precipitation and temperature in the Mediterranean area

E. Hertig · J. Jacobeit

Abstract The objective of this study is to investigate the predictability of monthly climate variables in the Mediterranean area by using statistical models. It is a well-known fact that the future state of the atmosphere is sensitive to preceding conditions of the slowly varying ocean component with lead times being sufficiently long for predictive assessments. Sea surface temperatures (SSTs) are therefore regarded as one of the best variables to be used in seasonal climate predictions. In the present study, SST-regimes which have been derived and discussed in detail in Part I of this paper, are used with regard to monthly climate predictions for the Mediterranean area. Thus, cross-correlations with time lags from 0 up to 12 months and ensuing multiple regression analyses between the large-scale SST-regimes and monthly precipitation and temperature for Mediterranean sub-regions have been performed for the period 1950–2003. Statistical hindcast ensembles of Mediterranean precipitation including categorical forecast skill can be identified only for some months in different seasons and for some individual regions of the Mediterranean area. Major predictors are the tropical Atlantic Ocean and the North Atlantic Ocean SST-regimes, but significant relationships can also be found with tropical Pacific and North Pacific SST-regimes. Statistical hindcast ensembles of Mediterranean temperature with some categorical forecast skill can be determined primarily for the Western Mediterranean and the North African regions throughout the year. As for precipitation the major predictors for temperature are located in the tropical Atlantic Ocean and the North Atlantic Ocean, but some connections also exist with the Pacific SST variations.

Keywords Monthly predictions · Mediterranean area · Sea surface temperature regimes · Statistical analyses

E. Hertig (✉) · J. Jacobeit
Institute for Geography, University of Augsburg,
Universitätsstr. 10, 86135 Augsburg, Germany
e-mail: elke.hertig@geo.uni-augsburg.de

1 Introduction

The interest in seasonal climate forecasts is due not only to scientific concerns but also to the high economic and social significance of this subject. In case of an adequate skill, the predictions can provide a basis for the development of adaptation strategies to climatic risks, e.g. in the field of water resources, stock-keeping, or crop diversification. Especially in regions like the Mediterranean area which are characterized by pronounced inter-annual climate variability and at the same time by manifold kinds of human land use, seasonal climate forecasts get particular importance.

Generally, two approaches are currently used for seasonal predictions. On the one hand, dynamical techniques are applied which are based on coupled atmosphere-ocean general circulation models (AOGCMs) or on atmosphere-only GCMs forced by independently predicted SSTs. Often the GCM output is further processed with dynamical or statistical downscaling techniques to improve the spatial resolution. On the other hand, multivariate statistical techniques are used from the very beginning, mostly based on multiple regression analysis and canonical correlation analysis. Sometimes, further methods like autoregression, discriminant analysis, particular approaches of time series analysis, or neural networking are applied to seasonal forecasts. The ability of these manifold dynamical and statistical techniques to predict seasonal climate strongly

depends on the particular region being analysed. Overall, most skilful seasonal predictions are achieved for the ENSO (El Niño-Southern Oscillation) phenomenon and its associated teleconnections. An overview of ENSO prediction studies is provided by Latif et al. (1998). Different statistical techniques, regarding their prognostic skill for El Niño-events, are compared by Mason and Mimmack (2002).

Tropical SSTs reveal a relatively strong coupling with the atmosphere, best reflected in the ENSO-system. But with respect to remote influences, van Oldenborgh (2005) notes that in winter linear correlations of the Niño-3 index and 500 hPa geopotential heights over Europe are very low. In contrast to that, Pozo-Vasquez et al. (2005) identify a potential predictability of wintertime precipitation in Europe and the Mediterranean area in dependence of Pacific El-Niño events. Mariotti et al. (2002) find that western Mediterranean rainfall is significantly correlated with ENSO during spring (negative sign) and autumn (positive sign). Brönnimann et al. (2007) point out by using long time series that in winter the response to El Niño is a negative North Atlantic Oscillation index, positive temperature anomalies in Turkey, as well as positive and negative precipitation anomalies in the western and southeastern Mediterranean area, respectively. They also find that the signal in Europe is strong when the Pacific Decadal Oscillation of the previous winter is in phase with ENSO.

The impact of extratropical SSTs, however, is controversially discussed. They exhibit significant variability at inter-annual timescales, and the identification of impacts on the atmosphere is hampered by the large internal variability of the latter. Nevertheless, Colman and Davey (1999) estimate European temperature and precipitation in summer from preceding winter SSTs of the North Atlantic Ocean using regression analysis. Rodriguez-Fonseca et al. (2006) find significant links of North Atlantic SSTs to winter precipitation in Europe and North Africa. The study of Rodwell et al. (1999) suggests an oceanic forcing on the large-scale atmospheric circulation in the North Atlantic area, particularly associated with the North Atlantic Oscillation (NAO). Also Czaja and Frankignoul (1999) found a relationship between a winter NAO-like pattern at the 500 hPa level and the North Atlantic SST variations with lead times for the latter of 3–5 months. Drévillon et al. (2001) suggested a connection between summer SSTs in one part of the Atlantic Tripole and the storm tracks over Europe during winter. Using lag-SVD (singular value decomposition) Rodriguez-Fonseca and Castro (2002) obtain a robust connection of summer North Atlantic SSTs and wintertime precipitation of the Iberian Peninsula and western North Africa. Despite such observed relationships, correct predictions of large-scale dynamical regimes remain difficult. Using the DEMETER models (Development of a European multi-model ensemble system for seasonal to inter-annual prediction, Palmer et al. 2004), the predictability of dynamical regimes (like the NAO) receives low scores, even though the winter monthly pressure fields and temperature impacts are correctly simulated (Fil and Dubus 2005).

The skill of direct DEMETER precipitation forecasts strongly fluctuates from season to season. Highest skills are reached for Spain in early and late spring, summer, and autumn with zero- and one-month lead times. For winter there is poor skill with the exception of the El Niño period 1986–1988 (Díez et al. 2005). Pavan et al. (2005) have downscaled DEMETER winter seasonal hindcasts over Northern Italy using multiple linear regression to obtain highly resolved fields for precipitation, minimum and maximum temperature. They obtain satisfactory forecast skill with best performance for maximum temperature. Frías et al. (2005) studied the predictability of monthly average maximum temperatures over the Iberian Peninsula using DEMETER simulations and downscaling, they conclude that predictability is very small and limited to the winter months.

In general, however, dynamical approaches as well as statistical techniques show relatively low skill in predicting seasonal precipitation and temperature for Europe and the Mediterranean area. But both methods benefit from the incorporation of oceanic information in the forecast models, even so there are striking uncertainties in many cases how particular SST signals are transferred over the atmospheric circulation onto regional precipitation patterns. In the region of Europe and the Mediterranean area, teleconnections from the adjacent Atlantic Ocean up to the tropical Pacific Ocean have been identified with different signals interfering with each other.

In view of the fact that SSTs are one of the most important variables for seasonal climate variability with observational data sets of comparatively good quality and widespread coverage, the present study concentrates on statistical relationships between SSTs and regional precipitation and temperature being relevant for seasonal predictions at a monthly time scale. Three particular aspects have to be mentioned in this context: (1) the oceanic predictors have been condensed to so-called SST regimes (see part I of this paper) which are determined for all ocean basins between 20°S and 60°N allowing to consider remote teleconnections, too. (2) The monthly predictions of Mediterranean precipitation and temperature are not derived for a single region, but for various subregions of similar rainfall variability and similar temperature variability, respectively (see Sect. 3). Thus, it is possible to compare the seasonal predictabilities for these different sub-regions within the entire Mediterranean area.

(3) The monthly forecasts are based on interannual stationary relationships between the large-scale oceanic variability and Mediterranean climate variables. Changes of these relationships due to e.g. decadal climate variations or global warming are not considered in this context.

Statistical techniques include cross correlation and multiple regression analyses which are specified in Sect. 4 together with appropriate assessments of forecast performance. Section 5 includes an overview of results as well as two particular examples for regional precipitation which are discussed in more detail. Section 6 contains the corresponding information for regional temperature.

2 Data

Monthly Mediterranean precipitation and temperature data are taken from a revised version of the global CRU05 dataset [Climatic Research Unit (CRU) in Norwich, New et al. 1999, 2000]. The data set comprises monthly values on a 0.5° × 0.5° grid for terrestrial areas, based on station data from the World Meteorological Organization, National Weather Services, and the CRU archives. The revision includes homogenizations and an update of the original dataset, performed by the Potsdam Institute for Climate Impact Research (PIK), see Oesterle et al. (2003).

Grid boxes indicating a characteristic Mediterranean precipitation regime are selected from the global data set as described in detail by Hertig (2004). Grid boxes with completely lacking precipitation in a particular month during the study period 1950–2003 are excluded from further analysis. This concerns grid boxes in southern and in eastern parts of the Mediterranean area in the summer half year. Thus, 1,169 grid boxes (July) up to 1,366 grid boxes (winter half year) are maintained from the selected data set.

To set the boundaries of the Mediterranean area for the temperature analysis, all grid boxes between 29°N and 45.5°N and from the North Atlantic coast to 40°E are selected from the global data set, thus covering mainly the radiation climate zone of the lower mid-latitudes. Altogether 2,363 grid boxes are representing the Mediterranean land areas.

The starting year (1950) of the following analyses results from the availability of high-quality SST-data, the ending year (2003) has been the last complete year at the beginning of this investigation.

3 Mediterranean precipitation and temperature regions

S-mode (Richman 1986), orthogonally (Varimax) rotated principal component analysis (PCA, e.g. Preisendorfer 1988; von Storch and Zwiers 1999) has been separately applied to monthly Mediterranean precipitation and temperature fields in order to remove linear dependencies between variables and to reduce dimensions of the data. Correlation analysis of temperature fields of successive months shows that the strongest relationship exists between temperature in July and temperature in August with a correlation coefficient of 0.45 averaged over the whole Mediterranean area. Correlation analysis of precipitation fields reveals that there are only very low correlations from one month to the next. The strongest relationship exists between July and August precipitation and between February and March precipitation with a mean correlation coefficient for the whole Mediterranean area of only 0.18. Therefore, PCAs (and all subsequent analyses) are performed with monthly mean instead of seasonal values. This means that the forecast period (validity period of the forecasts) is 1 month.

The determination of the number of PCs corresponds to the procedure already described in Sect. 3 of Part I of this paper with respect to the determination of sea surface temperature regimes. Depending on the analysed month, precipitation fields are reduced to 9 (February) or up to 19 PCs (June, August) with overall explained variances (EVs) between 71 and 79%. Temperature fields are reduced to 4–6 PCs with overall EVs between 76 and 86%.

S-mode loadings cluster the grid boxes with similar temporal variation in rainfall or temperature, and only the larger absolute loadings are interpretable. The s-mode scores are standardized time series that correspond well to those grid boxes with high absolute PC loadings (Compagnucci and Richman 2008). Thus, the illustration of the higher absolute loadings indicates the spatial centres of similar rainfall or temperature variation and allows for the delimitation of so-called precipitation and temperature regions, respectively. As an example Fig. 1 shows the Mediterranean precipitation and temperature regions for January. They are defined by PC loadings greater than 0.5 for precipitation and greater than 0.6 for temperature. These thresholds were used because they lead to non-overlapping regions covering the Mediterranean area almost entirely.

4 Hindcast model build-up

4.1 Cross-correlation analyses

Cross-correlation analyses between the time coefficients (s-mode PC scores) of all 17 SST regimes described in part I of this paper and the Mediterranean precipitation and temperature regions are carried out with lead times of the former from 0 (simultaneous link) up to 12 months. This is

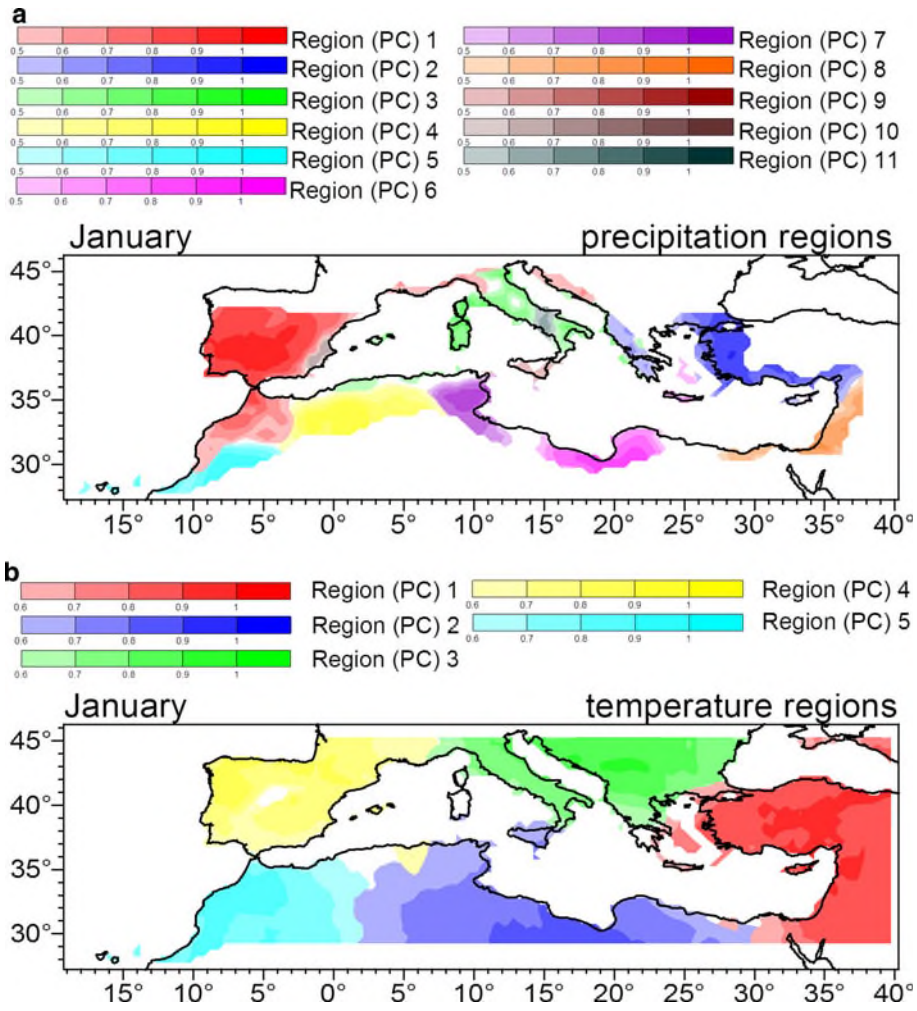

Fig. 1 **a** Mediterranean regions of similar precipitation variability in January defined by PC loadings greater than 0.5 of the s-mode PCA of Mediterranean monthly precipitation in the period 1950–2003. **b** Mediterranean regions of similar temperature variability in January defined by PC loadings greater than 0.6 of the s-mode PCA of Mediterranean monthly temperature in the period 1950–2003

done in order to pre-select predictor variables for subsequent multiple regression analyses.

From the large pool of bivariate cross correlation coefficients (for precipitation (temperature) a minimum of more than 1,800 (800) coefficients per month, derived from correlations between 9 and 19 precipitation regions (4–6 temperature regions) and 17 SST regimes considering 12 time lags), the significant coefficients (99% level of significance, absolute amount greater than 0.36 in case of a sample size of 50) are used to select the independent variables for subsequent multiple regression analyses. Summed up over all precipitation regions, between 41 (January) and 86 (August) significant correlations per month can be found among all coefficients described above. For the temperature regions, the corresponding number varies between 20 (December) and 30 (April). The maximum amount of cross correlation coefficients is around 0.7. For each month and each precipitation/temperature region the time coefficients of those SST-regimes showing a significant cross correlation to the rainfall/temperature of that region, are taken as predictor variables for the next step.

4.2 Multiple regression analyses with cross-validation procedure

In a first step, for each sub-period and each precipitation/temperature region a stepwise multiple regression procedure (von Storch and Zwiers 1999, p. 166) is applied which combines forward selection with backward elimination. The *F* test is used for entering and maintaining variables in the regression equation, using significance levels of 0.05 and 0.10, respectively. Further diagnostic procedures are used to examine the residuals with respect to normal distribution (Shapiro–Wilk Test, see Royston 1982), serial correlation (Durbin–Watson statistic, see von Storch and Zwiers 1999, p. 157), and heteroscedasticity (Breusch–Pagan-Test, see Breusch and Pagan 1979). To ensure that the regression models are adequate, tests for the multiple correlation coefficients (*F* test with a significance level of

0.05), and tests for the partial regression coefficients (t test with a significance level of 0.05) have been performed (von Storch and Zwiers 1999, p. 150).

Validation of models which are designed for seasonal forecasts should be done in a cross-validation framework. Basic rules for cross-validation imply that every detail of the statistical calculations has to be repeated, including re-definition of climatology and anomalies. The predictors and predictands of the verification sub-period must not be serially correlated with their counterparts in the period used for model build-up. Therefore, the cross-validation procedure in the present study has been done as follows: at first five consecutive years are removed from the complete sample. Then a statistical model is generated with the remaining years (54–5 = 49 for the period 1950–2003) and applied to make a statistical forecast to be verified for the central year of the removed 5 year period. Subsequently, the removed years are replaced and the whole procedure is repeated for a different group of years until the hindcast verification sample comprises 18 models. The replaced years are selected by means of a random generator. In general, cross-validation allows the entire sample to be used for verification, but in view of the large number of different forecast configuration tests, one-third of the sample size is thought to be sufficient in the present context.

The regression models from the hindcast verification sample are used for an improved selection of predictors. This is done by counting how often a certain independent variable (SST-regime) is selected in the 18 regression equations for a particular precipitation/temperature region. Only those independent variables which are predominantly selected in the stepwise regression models (minimum of 12 models corresponding to at least two-thirds of all models) are taken for further analysis. This means that multiple regression is applied a second time, but now with fixed predictors and without a stepwise selection of the independent variables. The regression models with the fixed predictor set are also submitted to the above-mentioned diagnostics, and those models which meet the requirements are combined to a statistical model ensemble. Its forecast skill has to be evaluated by means of appropriate quality criterions which will be discussed in Sect. 4.3.

4.3 Hindcast models and forecast performance

Long range forecasts should be verified in hindcast mode to give an accurate assessment of their skill by the use of a larger number of available verification years. Moreover, verification in hindcast mode should be done preferably in the same way as the real time operating mode in terms of resolution, ensemble size and involved parameters. For the skill assessment of a forecast model the correlation coefficients between predicted and observed values can be used. They allow for inferences of phase errors, but ignore biases and scale errors in the forecasts (Murphy and Epstein 1989). Therefore, other verification tools are necessary to assess the forecast performance. A commonly used model verification measure is the root mean squared skill score relating the forecast errors to the errors of a reference forecast (e.g. persistence or climatology). The RV-value (reduction of variance) is similar to the root mean squared skill score:

$$\mathrm{RV} = \left(1 - (\mathrm{rmse}_1/\mathrm{rmse}_2)^2\right) \times 100[\%]$$

rmse_1 = root mean squared error of forecast rmse_2 = root mean squared error of reference (in this study climatology, because of extratropical forecasts)

A RV-value of 100% means a perfect forecast, RV > 0% indicates an improvement of the results, whereas RV = 0% implies that there is no improvement compared to the simple use of the reference forecast.

However, results in this study are mostly presented in terms of three-category forecasts classifying into below normal, near normal and above normal values. The threshold values for these classes are the limits of the confidence intervals for the long-term mean at the 10% significance level (using Student's t distribution). Generally, at least about 90 forecast/observation pairs are required to properly estimate a three-by-three contingency table. Thus, it is recommended by the World Meteorological Organization (2007) that the provided tables should be aggregated over windows of target periods or over verification points. In the present study, an aggregation over the grid boxes belonging to a particular precipitation/temperature region as well as over the 18 verification years belonging to a forecast ensemble has been chosen, thus ensuring that the required number of forecast/observation pairs is achieved in any case. For the categorical forecasts in terms of three-by-three contingency tables, an appropriate skill score is provided by Gerrity (1992), the Gerrity Skill Score (GSS).The definition of GSS uses a scoring matrix $s_{i,j}$ ($i, j = 1,\ldots,3$) being a tabulation of the reward or penalty of every forecast/observation outcome. Rare events are more rewarded in case of a correct forecast and less penalized in case of an incorrect forecast, whereas common events are lesser rewarded and stronger penalized. A positive GSS means that the forecast is better than assuming future conditions will be similar to the long-term average. It has to be noted that there is an analysis bias if the outcome is very unequally distributed in the table's categories. But GSS has many advantages like its ease of construction, its objectiveness, and its weighted calculation.

5 Forecasts of regional Mediterranean monthly precipitation

From the analysis of the regional Mediterranean precipitation in all months of the year it has to be concluded that long-term forecasts are only possible for a few regions of the Mediterranean area in selected months. Relationships of SST-Regimes and Mediterranean precipitation in particular regions can only be found from August to March. In the remaining months, from April to June, no successful seasonal forecast models can be established. Models are called 'successful' if some skill becomes evident in the categorical precipitation forecasts according to the Gerrity Skill Score (see Sect. 4.3). The GSS lies in the range from 0.1 up to about 0.8, with the highest value for the categorical forecast of September precipitation in the western Iberian Peninsula. The ensemble mean correlation coefficient for the hindcast years lies in the range of about 0.4–0.5, the ensemble mean bias at about 3 mm/month up to 15 mm/month. However, the probabilistic forecasts (without categorization) do not show a positive RV-value for a whole hindcast ensemble, only individual years exhibit a positive skill. This means that the probabilistic forecast ensembles do not provide an improvement compared to the simple reference of the long-term mean values. Despite this negative skill of the probabilistic forecasts, a viable prediction is possible when using categories as discussed above.

Successful modelling has been performed for the following months and regions:

- January precipitation in the Mediterranean parts of Libya. The SST-regimes which are selected as predictors are the Indian Ocean Regime I in May/June and the Atlantic Ocean Regime III in November/December (for loading patterns see Fig. 2 in part I of this paper also including short characterizations in Sect. 5). The skill of the categorical forecast is quite low with GSS = 0.09.
- February precipitation in the Atlas Mountains of Morocco. Model predictor is the Atlantic Ocean Regime IV in June–August. The skill is quite low again with GSS = 0.10.
- March precipitation in the northeastern Mediterranean region around the Aegean Sea (details in Sect. 5.1).
- August precipitation in the highlands of the central Iberian Peninsula (approximately between the Cantabrian Mountains in the North and the Castilian Mountains in the South, details in Sect. 5.2).
- September precipitation in the western parts of the Iberian Peninsula (details in Sect. 5.2).
- October precipitation in the northeastern Mediterranean region around the Aegean Sea. Forecast predictors are the Pacific Ocean Regime II in April and the Pacific Ocean Regime VII in February/March with GSS = 0.72.
- November precipitation in the southeastern Mediterranean region (parts of Egypt, Israel, Lebanon, and Syria). Once again the Pacific Ocean Regime VII is involved, now with its time series of the preceding December. In addition, another tropical regime is incorporated, the Atlantic Ocean Regime I in November/December. The skill is quite low with GSS = 0.14.
- December precipitation in the Iberian Peninsula area. Forecast predictors are the Atlantic Ocean Regime I in June and the Indian Ocean Regime I in April. The skill of the categorial forecast amounts to GSS = 0.38.

To specify in detail the statistical regime-climate-relationships providing the basis of a successful forecast, two examples are selected and discussed in the following subsections.

5.1 March precipitation in the northeastern Mediterranean region

This region covers the areas around the Aegean Sea (western Turkey and eastern Greece, see Fig. 2a). The prototypical loading patterns of the SST-regimes which are selected as predictors for March precipitation in this region, are shown in the left panels of Figs. 2b, c. The corresponding cross-correlation coefficients between SST-regime and regional precipitation are plotted in the right panels of Figs. 2b, c (arrows indicate which time series of the regime is selected in the multiple regression equations). Two SST-regimes are selected as predictors for March precipitation. The Atlantic Ocean Regime II (for a characterisation see Sect. 5.2 of part I of this paper) shows higher cross-correlation coefficients with no time lag and with the preceding winter anomaly, at relatively short lead times of up to about 4 months (right side of Fig. 2b). In the regression equations underlying the March forecasts, the regime specification of December–February is chosen as independent variable. The second SST-regime which is included in the regression models, is the Pacific Ocean Regime III (description see Sect. 5.1 of part I), showing a mixed picture regarding the cross-correlation coefficients (right side of Fig. 2c). There are weak negative coefficients with no time lag, otherwise mainly positive ones. In the regression equations, the regime specification of September–November is selected as predictor for March precipitation. Altogether, northeastern Mediterranean March precipitation depends on particular North Atlantic and North Pacific SST configurations in the previous winter and autumn seasons, respectively. Thus, the oceanic patterns in the upstream areas in preceding seasons support a specific

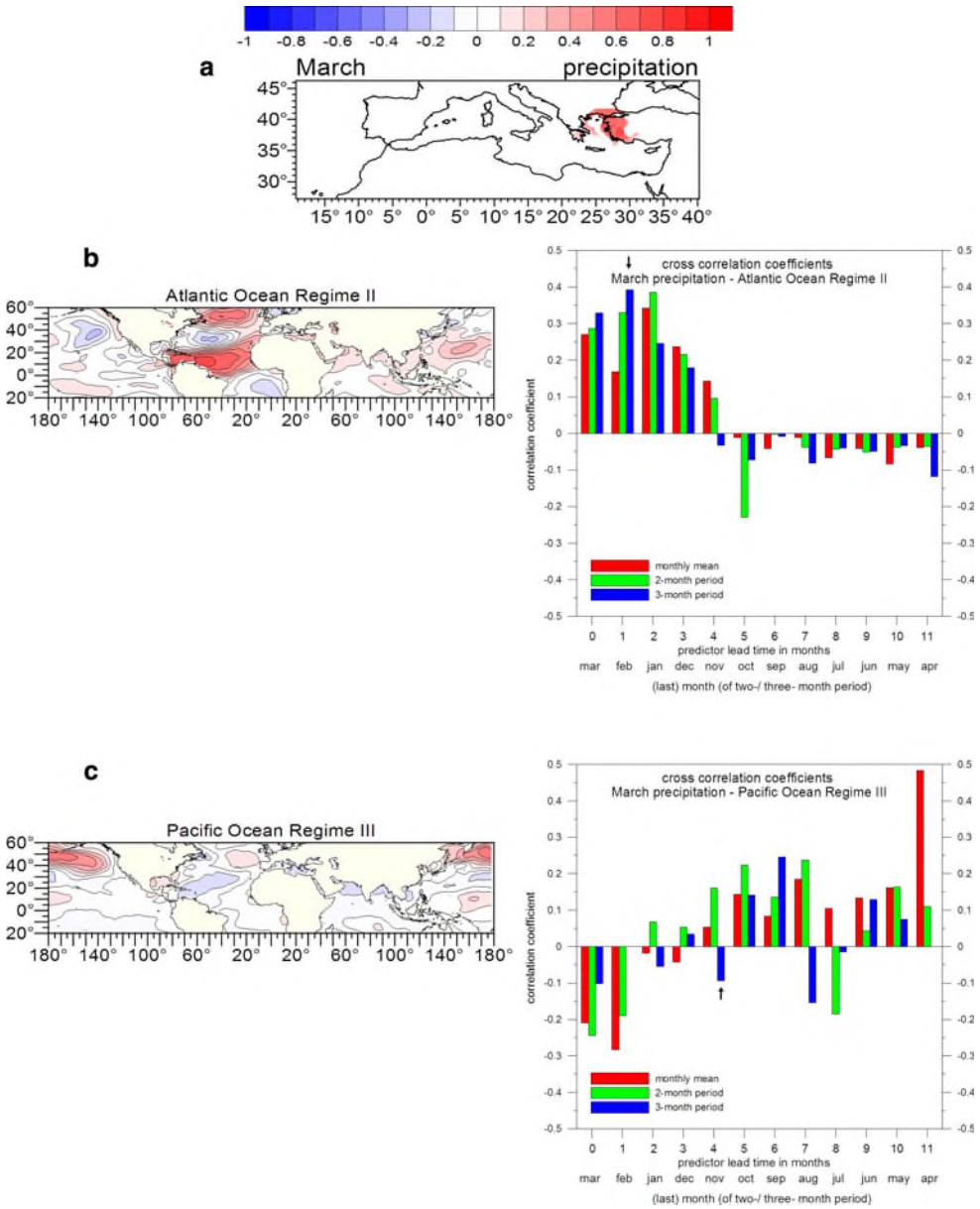

Fig. 2 Relationships of SST-regimes and Mediterranean precipitation. **a** Location of the analysed region (western Turkey and eastern Greece, area marked with *red* colour). **b**, **c** *Left side* Prototypical loading patterns of the SST-regimes which are selected as predictors for northeastern Mediterranean precipitation in March. **b**, **c** *Right side* Corresponding cross-correlation coefficients of the SST-regime scores and regional precipitation. The *arrows* indicate which time series of the regimes are selected in the multiple regression equations

large-scale atmospheric flow in spring which influences precipitation in the target region.

Relationships are further specified by Table 1 showing the cases with positive (scores ≥ 0.7) and negative (scores ≤ -0.7) modes of the Atlantic Ocean Regime II from December to February in reference to below normal, near normal and above normal northeastern Mediterranean precipitation in the subsequent month of March for the 1950–2003 period. It reveals that in average over all grid boxes of the region (130) in nearly nine out of twelve cases with the negative mode of the SST-regime below normal precipitation occurs, whereas in about five out of thirteen cases with the positive mode of the SST-regime above normal precipitation follows. It has to be mentioned that

Table 1 Cases of positive (scores ≥ 0.7) and negative (scores ≤ -0.7) modes of the Atlantic Ocean regime of Fig. 2b from December to February with respect to below normal, near normal and above normal precipitation in the northeastern Mediterranean region (see Fig. 2a) in the subsequent month of March

	Negative mode of SST-regime	Positive mode of SST-regime
Below normal precipitation	8.9	4.9
Near normal precipitation	1.1	2.7
Above normal precipitation	2	5.4
Sum	12	13

The threshold values for the precipitation classes are the limits of the confidence interval for the long- term mean at the 10% significance level (using Student's *t* distribution)

the corresponding contingency coefficient of Table 1 is not significant (Chi-square distributed test statistic, Bahrenberg et al. 1999). Nevertheless, the strong relationship of the negative SST mode and below normal precipitation is striking.

Looking at composites of the 1,000 hPa-geopotential heights in the forecast month of March (Fig. 3), calculated from those cases when the Atlantic Ocean Regime II is in its negative (positive) mode from December to February and regional precipitation is below (above) normal in the subsequent month of March, it becomes evident that in the first case the negative SST mode favours relatively strong anticyclonic conditions over central Europe and most parts of the Mediterranean area (upper part of Fig. 3). This is connected with a dry anticyclonic flow from easterly directions into the Aegean region. In the second case, above normal SSTs in the western North Atlantic Ocean around 10°N and 50°N and below normal SSTs around 30°N from December to February promote a low pressure system north of the British Isles 1 month later whose extensions reach as far as the northeastern Mediterranean area (lower part of Fig. 3). Thus, cyclonic conditions lead to above normal precipitation in this region. It has to be mentioned that with the occurrence of the positive SST mode the other precipitation categories (below normal and near normal) occurred more often than above normal precipitation (see right column of Table 1). This indicates that the positive SST mode does not exert a clear linear effect on precipitation. In contrast to that, the relationship of the negative SST mode to below normal precipitation is dominant, so that some kind of non-linearity becomes evident in the SST-precipitation-relationships.

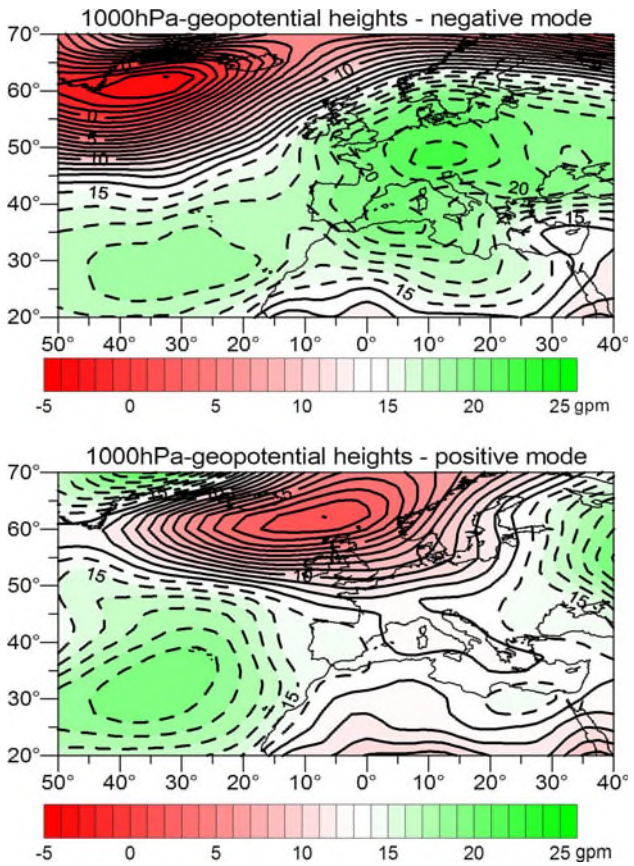

Fig. 3 Composites of the 1,000 hPa-geopotential heights in the forecast month of March, calculated from those cases when the Atlantic Ocean Regime II of Fig. 2b is in its negative (positive) mode from December to February and precipitation in the Aegean Region (see Fig. 2a) is below (above) normal in the forecast month of March - see *upper* (*lower*) *panel*

The prediction of below normal precipitation benefits from a relatively strong influence from the North Atlantic Ocean in the previous months. This can also be seen in Table 2 depicting the categorical forecast results for March precipitation in the Aegean region. Almost all of the observed below normal precipitation events have correctly been predicted (432 correct cases out of 451 observed cases with below normal precipitation). Additionally Table 2 indicates that 878 near normal events and 184 above normal events have correctly been predicted, whereas in 539 cases the near normal conditions according to observation are overestimated as above normal precipitation in the forecast ensemble. From the contingency table a GSS = 0.41 arises, so that the forecast ensemble still performs quite well for the prediction of March precipitation in the northeastern Mediterranean area. But it has to be considered that the forecast lead time is at its minimum, because the SST regime for December–February is taken for the prediction of precipitation in March. The RV-value of the best performing model is 34.77% for the forecast of March 1960. The ensemble mean correlation coefficient is 0.395, and the ensemble mean bias of the forecast amounts to 7.9 mm for the whole precipitation region.

Table 2 3 × 3-contingency table of the forecast ensemble (18 ensemble members) of northeastern Mediterranean precipitation in March (130 grid boxes, location of the region see Fig. 2a)

GSS:0.41	Observation		
	Below normal	Near normal	Above normal
Forecast			
Below normal	432	180	72
Near normal	19	878	36
Above normal	0	539	184

The threshold values for the precipitation classes are the limits of the confidence interval for the long- term mean at the 10% significance level (using Student's *t* distribution)

GSS Gerrity skill score

5.2 September precipitation in the western Iberian Peninsula

The exact location of the region is indicated in Fig. 4a. Three SST-regimes are selected as predictors in the multiple regression models, first of all the Atlantic Ocean Regime II (left side of Fig. 4b). This regime shows weak negative cross-correlation coefficients with September precipitation in parts of the Iberian Peninsula with no and shorter lead times. In the preceding spring, the sign of the correlation coefficient changes, and a maximum positive correlation of about 0.45 arises for the SST-regime

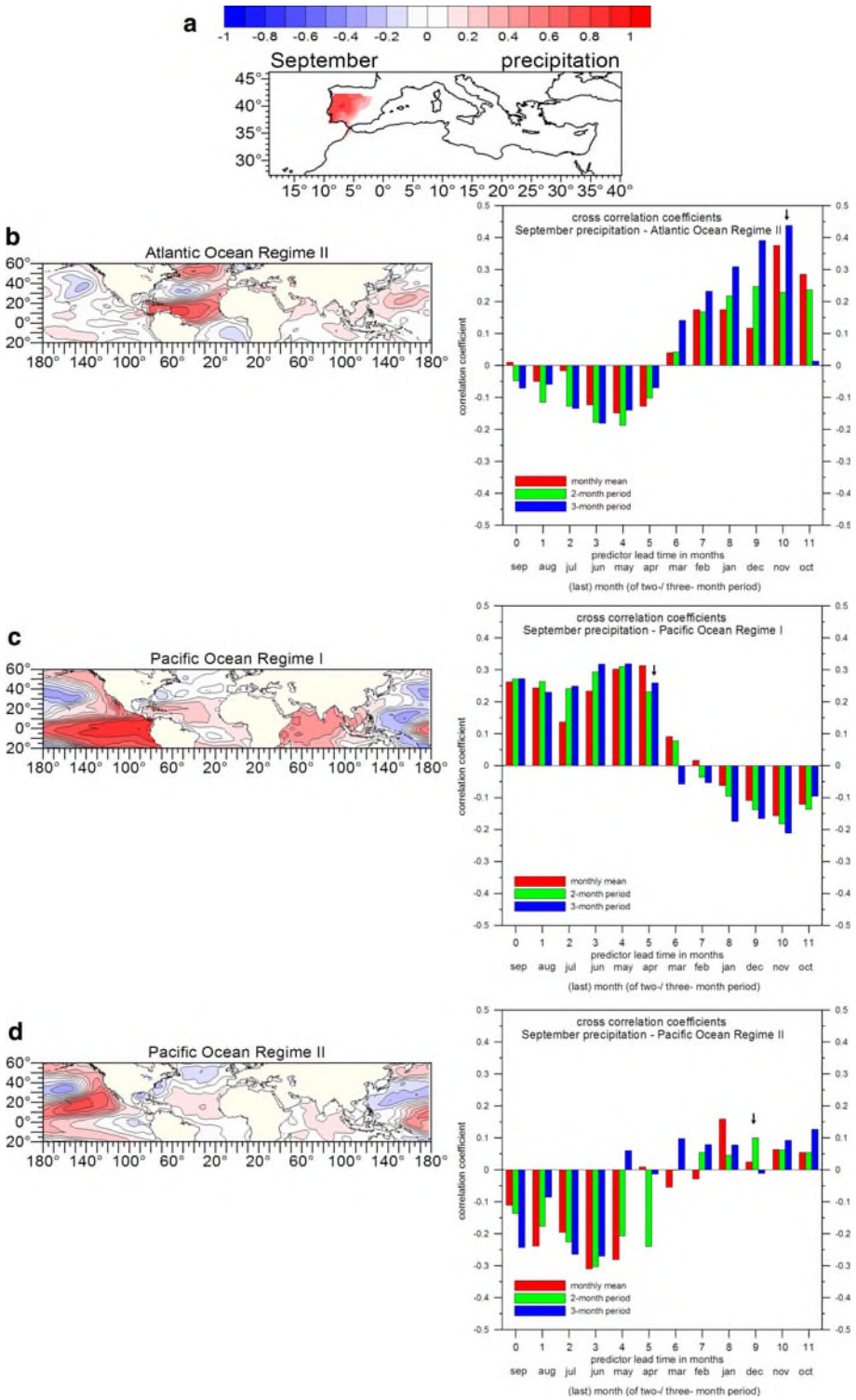

Fig. 4 Relationships of SST-Regimes and Mediterranean precipitation. **a** Location of the analysed region (western and central parts of the Iberian Peninsula, area marked with *red* colour).**b–d** *Left side* Prototypical loading patterns of the SST-regimes which are selected as predictors for precipitation in September in parts of the Iberian Peninsula. **b–d** *Right side* Corresponding cross-correlation coefficients of the SST-regime scores and regional precipitation. The *arrows* indicate which time series of the regimes are selected in the multiple regression equations

configuration of September–November of the previous year (right side of Fig. 4b). This configuration is also incorporated in the forecast models.

Beside the Atlantic Ocean Regime II two further regimes having their centres of variation in the Pacific Ocean, are taken as predictors. The first one is the Pacific Ocean Regime I which reflects the El Niño phenomenon (left side of Fig. 4c). The corresponding cross-correlation coefficients with September precipitation on the right side of Fig. 4c include positive signs with no and short lead times. In the preceding spring, the sign of the coefficients switches to negative. Interestingly, the time series with the highest cross-correlation coefficient is not incorporated in the regression equations, but instead another one which lies at the turning point from positive to negative correlations. Therefore, it is important how the centre of variation in the tropical eastern Pacific is developed during February to April, the time when the ENSO-system is reorganized. Mariotti et al. (2002) find a higher autumn correlation for western Mediterranean precipitation with the Nino3.4 indices immediately before the mature phase of ENSO, whereas the significant winter and spring signals are during and after the mature phase of an ENSO event. In the present study, however, it becomes evident that the relatively weak correlations in the developing stage of El Niño or La Niña episodes in the spring and summer months can well be used for September precipitation forecasts.

Gualdi et al. (2003) suggest that the North Atlantic variability only shows a connection to La Niña-events, but not to El Niño ones. Pozo-Vasquez et al. (2001) and Cassou and Terray (2001a, 2001b) also point out that the ENSO influence on the North Atlantic/European region is found to be stronger during cold events. Possible mechanisms may involve effects of the PNA and NAO patterns and the influence of ENSO-related tropical Atlantic SST anomalies. Zanchettin et al. (2008) further point out that El Niño/La Niña-events exhibit a significant influence on rainfall in the western parts of Europe under weak phases of the NAO, whereas a strong NAO suppresses the ENSO signal. Looking at Table 3—relating the cases with the positive (scores ≥ 0.7) and negative (scores ≤ -0.7) modes of the Pacific Ocean Regime I from February to April to below normal, near normal and above normal September precipitation in parts of the Iberian Peninsula—reveals that (averaged over all grid boxes of the region) in 8.6 out of 11 cases of the negative SST-mode (La Niña) in the 1950–2003 period, below normal precipitation subsequently occurs. In contrast to that, only for half of the cases with the positive SST-mode (El Niño) above normal precipitation can be observed (right side of Table 3). Like for March precipitation in the northeastern Mediterranean area, the contingency coefficient is not significant. Nevertheless, the present study confirms that the link of cold SST events to regional precipitation is stronger than the connection for the positive SST mode.

The geopotential height composites (1,000 hPa level) of the same cases as in Table 3 reveal that below normal precipitation is connected to a high-pressure system with its centre above the eastern North Atlantic Ocean at around 40°N extending eastwards across almost the whole Mediterranean area (upper part of Fig. 5). Thus, negative anomalies of the centre of variation in the eastern tropical Pacific from February to April promote anticyclonic conditions over the North Atlantic/Mediterranean area in the subsequent autumn period of September. Additionally, the regression equations which are used for the seasonal forecasts, also include the Atlantic Ocean Regime II and the Pacific Ocean Regime II. The corresponding composites compiled with the modes of the Atlantic Ocean Regime II from September to November as well as with the modes of the Pacific Ocean Regime II from November to December yield similar results, showing anticyclonic conditions in the above- mentioned regions during September of the following year leading to below normal precipitation over parts of the Iberian Peninsula. In the opposite case with above normal precipitation the corresponding composites indicate different types of circulation anomalies: For instance the composite pattern for the positive mode of the Pacific Ocean Regime I exhibits a positive pressure anomaly over the British Isles and the North Sea and below normal pressure over the subtropical North Atlantic Ocean (lower part of Fig. 5). The Iberian Peninsula is located near to the transition zone between positive and negative geopotential height anomalies and affected by slightly above normal precipitation. However, the composite pattern for the positive mode of the Atlantic Ocean Regime II shows a pronounced negative anomaly over the North Atlantic Ocean west of the British Isles extending as far as the northwestern Mediterranean area (not shown) thus confirming favorable conditions for above

Table 3 Cases of positive (scores ≥ 0.7) and negative (scores ≤ -0.7) modes of the Pacific Ocean regime of Fig. 4c from February to April with respect to below normal, near normal and above normal precipitation in parts of the Iberian Peninsula (see Fig. 4a) in the subsequent month of September

	Negative mode of SST-regime	Positive mode of SST- regime
Below normal precipitation	8.6	3.3
Near normal precipitation	1.1	2.7
Above normal precipitation	1.3	6.0
Sum	11	12

The threshold values for the precipitation classes are the limits of the confidence interval for the long- term mean at the 10% significance level (using Student's *t* distribution)

normal precipitation over the Iberian Peninsula (9.6 out of 13 cases, calculated in correspondence to Table 3).

We may conclude from the various composite patterns that forecasts of below normal precipitation are rather connected to the negative mode of the tropical Pacific Ocean Regime I (ENSO) in spring, whereas above normal precipitation is related to the positive mode of the North Atlantic Ocean Regime II (North Atlantic Tripole) in the preceding autumn/early winter. The additional selection of the Pacific Ocean Regime II (left side of Fig. 4d) results from accounting for residual variance which is not yet explained in the regression models by the former two regimes. Other studies also show an additional influence of the North Pacific sector. For example, according to Zanchettin et al. (2008) and Brönnimann et al. (2007), positive phases of the PDO imply that strong ENSO events exert a more significant influence on European wintertime precipitation. Thus, the Atlantic Ocean Regime II (North Atlantic Tripole), the Pacific Ocean Regime I (ENSO) and the Pacific Ocean Regime II (non-ENSO North Pacific variability) act together in influencing September precipitation in parts of the Iberian Peninsula.

It should be mentioned in this context that precipitation in August in central parts of the Iberian Peninsula can also be successfully predicted by models including the Atlantic Ocean Regime II and the Pacific Ocean Regime II (GSS = 0.41). But as a third regime, instead of the Pacific Ocean Regime I (ENSO), the Atlantic Ocean Regime I is selected, pointing to a connection with tropical Atlantic SST variations.

According to Table 4 summarizing the results of the categorical forecast ensemble for September precipitation in parts of the Iberian Peninsula, 612 grid box predictions of above normal precipitation also occur in the observation. However, for 679 cases the forecasts are too wet (above normal precipitation predicted, but only near normal conditions observed). Nevertheless, the categorical forecast ensemble performs quite well with GSS = 0.76. The best performing model in terms of the RV-value is for September 1972 with RV = 26.5%. The ensemble correlation coefficient between forecast and observation is 0.443, and the ensemble mean bias amounts to 7.1 mm.

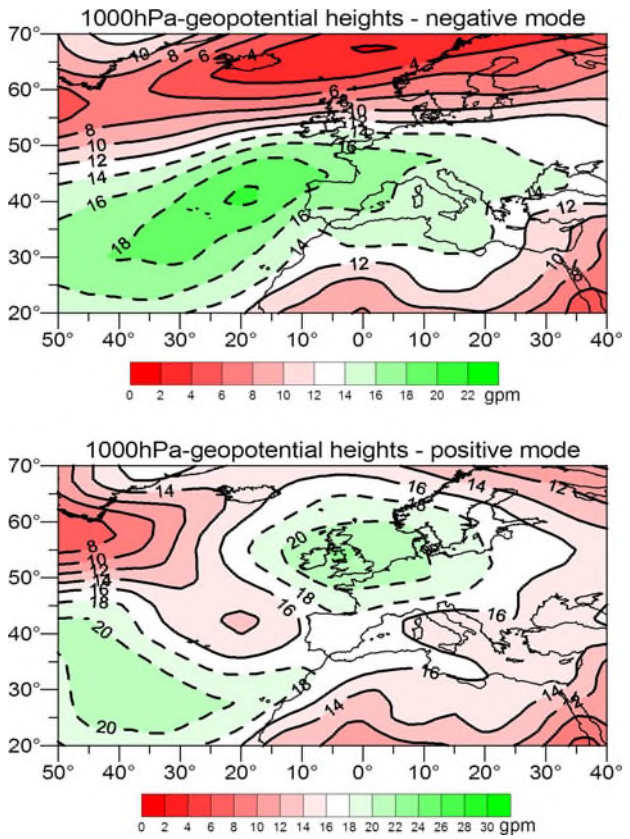

Fig. 5 Composites of the 1,000 hPa-geopotential heights in the forecast month of September, calculated from those cases when the Pacific Ocean Regime I of Fig. 4c is in its negative (positive) mode from February to April and precipitation in parts of the Iberian Peninsula (see Fig. 4a) is below (above) normal in the forecast month of September, see *upper* (*lower*) I

6 Forecasts of regional Mediterranean monthly temperature

The analysis of the regional Mediterranean temperature in all months of the year reveals that long-term forecasts are possible mainly for the regions in the southern and western parts of the Mediterranean area in selected months. The GSS for the temperature forecasts lies in the range from about 0.2 up to 0.6, with the highest value for the categorical forecast of August temperature in the western Mediterranean region. The ensemble mean correlation coefficient for the hindcast years lies in the range of about 0.4–0.6, the ensemble mean bias at about 0.1°C/month up to 0.8°C/month. Like for the precipitation forecasts, the

Table 4 3 × 3-contingency table of the forecast ensemble (18 ensemble members) of precipitation in September in parts of the Iberian Peninsula (143 grid boxes, location of the region see Fig. 4a)

GSS:0.76	Observation		
	Below normal	Near normal	Above normal
Forecast			
Below normal	54	324	52
Near normal	90	491	110
Above normal	162	679	612

The threshold values for the precipitation classes are the limits of the confidence interval for the long- term mean at the 10% significance level (using Student's *t* distribution)

GSS Gerrity skill score

probabilistic temperature forecasts do not show a positive RV-value for a whole hindcast ensemble, only individual years exhibit a positive skill. Based on the categorical forecasts successful modelling of monthly Mediterranean temperature has been performed for the following months and regions:

- May temperature in the central North African region (in the area of Algeria and Tunisia). The SST-regimes which are selected as predictors are the Pacific Ocean Regime III in August and the Atlantic Ocean Regime III in July of the previous year (for loading patterns see Fig. 2 in part I of this paper, for short characterizations see Sect. 5 in part I). The skill of the categorical forecast is GSS = 0.22.
- August temperature in the western Mediterranean region (details in Sect. 6.1).
- September temperature in the western Mediterranean region including the whole Iberian Peninsula, southern France and the western parts of Mediterranean North Africa. The predictors are the Pacific Ocean Regime III and the Pacific Ocean Regime VIII in March, as well as the Atlantic Ocean Regime I in July/August and the Atlantic Ocean Regime II in September–November of the previous year. The categorical forecast skill is GSS = 0.41.
- November temperature in the central-northern Mediterranean region. Three SST-regimes are selected as predictors: the Pacific Ocean Regime VII in November–January, the Pacific Ocean Regime IV in May–July and the Atlantic Ocean Regime III in April. The skill of the categorical forecast amounts to GSS = 0.36.
- December temperature in the western North African region (details in Sect. 6.2).

Like for precipitation, two selected examples of regional temperature forecasts will be discussed in more detail (Sects. 6.1 and 6.2).

6.1 August temperature in the western Mediterranean region

This region includes the Iberian Peninsula, southern France, and northern Morocco. The relationships described below are also indicated for temperature of the western and central parts of the Mediterranean North Africa, but for these regions the multiple regression equations do not meet the conditions described in Sect. 4.2 (i.e. the regression models with the prescribed predictor set do not pass the whole diagnostic procedure). Nevertheless, similar relationships to the SST-regimes can be seen for August temperature in the western Mediterranean region as well as in the western and central parts of Mediterranean North Africa.

Figure 6 illustrates the location of the region under consideration (area marked with red colour in Fig. 6a), the prototypical loading patterns of the SST-regimes which are selected as predictors (left side of Fig. 6b–d) and the corresponding cross-correlation coefficients between the SST-regime and August temperature (right side of Figs. 6b–d). The arrows in the latter part indicate which time series of the SST-regime is selected in the multiple regression equations. Three oceanic regimes are selected as predictors for western Mediterranean temperature in August. Two of them have their centres of variation in the adjacent North Atlantic Ocean, and one regime is selected which focuses on the SST variation in the western tropical Pacific. The Atlantic Ocean Regime III with its centre of variation in the eastern North Atlantic (representing the North Atlantic horseshoe pattern, left side of Fig. 6b) exhibits high positive cross-correlation coefficients (maximum of 0.67) with August temperature for no lead time and short lead times (right side of Fig. 6b). The correlations drop with increasing lags and change their sign in the preceding late winter/spring season, at lag times of about 6–7 months. With even longer lead times of the SST-regime higher negative cross-correlation coefficients (app. −0.6) are evident for the autumn anomaly during the year before. In the regression equations no time series with high cross-correlation coefficients are selected, but instead that one of March which lies around the beginning point of positive correlation coefficients between the SST-regime and August temperature. The other relevant Atlantic Ocean Regime IV has its centre of variation in the central North Atlantic Ocean at around 40°N (left side of Fig. 6c). This regime displays a somewhat opposite behaviour regarding the cross-correlation coefficients compared to the former regime with negative coefficients up to 5 or 6 month lags and positive ones with longer lead times of the SST-regime (right side of Fig. 6c). Once again, not the time series with the highest cross-correlation coefficient is selected in the regression equations, but the regime realisation at around the point of change in sign of the coefficients (in this case the time series of the December–February mean). For the Pacific Ocean Regime VII, displaying a centre of variation in the tropical West Pacific (left side of Fig. 6d), the highest cross-correlation coefficient with August temperature in the western Mediterranean region exists for the November/December-mean of the regime's time coefficient (right side of Fig. 6d). This time series is also selected in the regression equations.

Altogether, it can be assumed that for the relationships of August temperature with North Atlantic SSTs it is important whether a particular regime configuration can develop at the end of winter until spring, thus favouring specific atmospheric conditions in the target month about half a year later. Relationships are further specified by

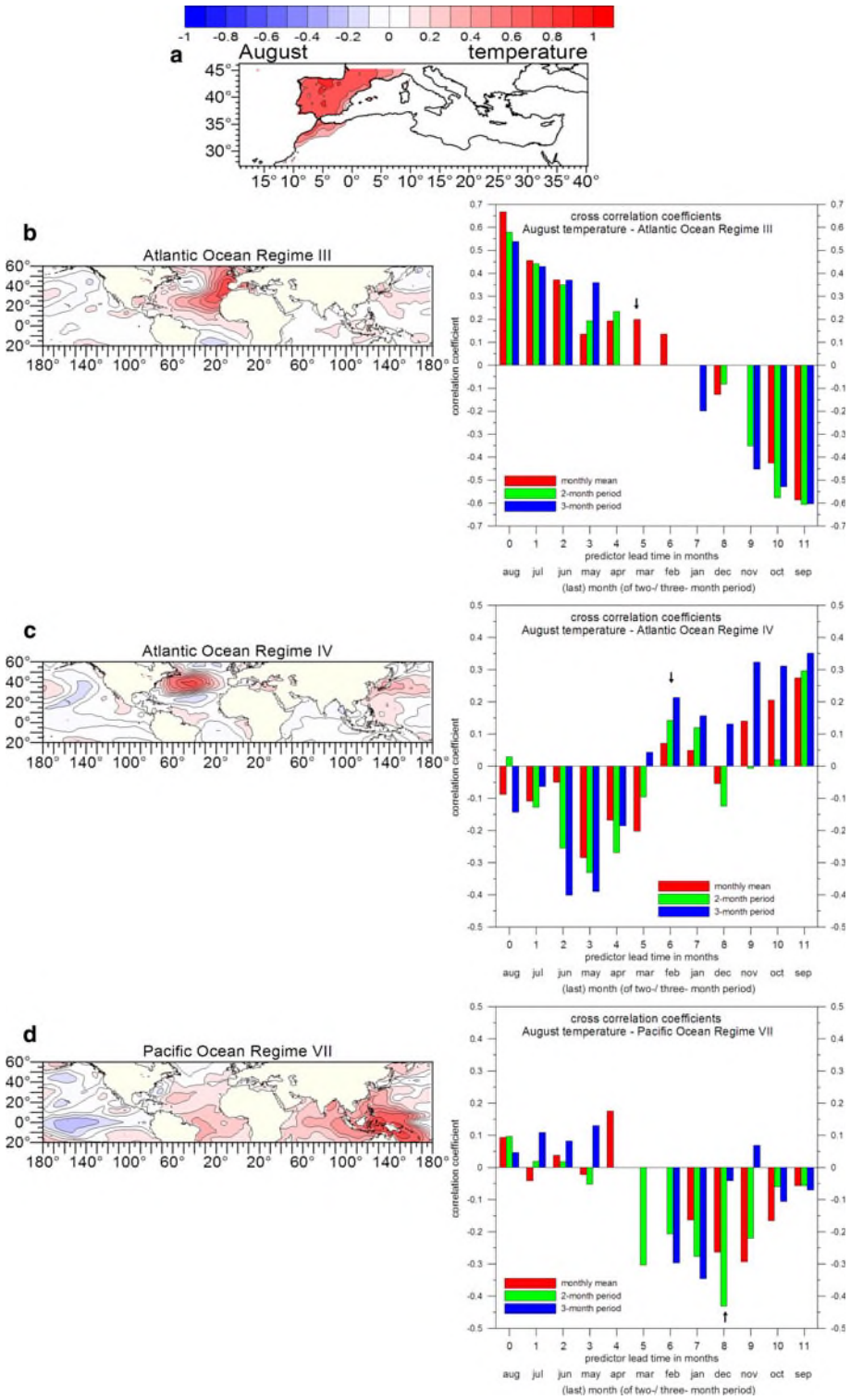

Fig. 6 Relationships of SST-Regimes and Mediterranean temperature. **a** Location of the analysed region (Iberian Peninsula, southern France, western North Africa, area marked with *red* colour). **b–d** *Left side* Prototypical loading patterns of the SST-regimes which are selected as predictors for temperature in August in the western Mediterranean region. **b–d** *Right side* Corresponding cross-correlation coefficients of the SST-regime scores and regional temperature. The *arrows* indicate which time series of the regimes are selected in the multiple regression equations

Table 5 showing the cases with positive (scores ≥ 0.7) and negative (scores ≤ -0.7) modes of the Atlantic Ocean Regime III in March in reference to below normal, near normal and above normal western Mediterranean temperature in the subsequent summer month of August. Averaged over all 489 grid boxes of the region, six out of eleven cases with the negative mode of the SST-regime are followed by below normal temperatures, whereas in about eight out of thirteen cases with the positive mode above normal temperatures are observed.

When looking at composites of the 1,000 hPa-geopotential heights in the forecast month of August (Fig. 7)—

Table 5 Cases of positive (scores ≥ 0.7) and negative (scores ≤ -0.7) modes of the Atlantic Ocean regime of Fig. 6b in March with respect to below normal, near normal and above normal temperature in the western Mediterranean region (see Fig. 6a) in the subsequent month of August

	Negative mode SST-regime	Positive mode SST-regime
Below normal temperature	5.8	3.2
Near normal temperature	2.3	1.9
Above normal temperature	2.9	7.9
Sum	11	13

The threshold values for the temperature classes are the limits of the confidence interval for the long- term mean at the 10% significance level (using Student's *t* distribution)

calculated from those cases when the Atlantic Ocean Regime III is in the positive (negative) mode in March and western Mediterranean temperature is above (below) normal in the subsequent month of August—it becomes evident that in the former case anticyclonic conditions prevail from the North Atlantic Ocean over the western Mediterranean area and Europe as far as eastern Europe (lower part of Fig. 7). Thus, the development of the positive SST mode in the eastern Atlantic Ocean at an early stage of the year favours anticyclonic conditions with above normal summer temperatures in the Iberian Peninsula, southern France and northern Morocco. In the opposite case, the negative SST mode in the eastern North Atlantic Ocean promotes relatively strong anticyclonic conditions being confined to the oceanic areas (upper part of Fig. 7). Meridional circulations from northerly directions in front of this anticyclone are responsible for below normal temperatures in the western Mediterranean area.

Table 6 summarizes the results of the categorical forecast. Obviously there is mainly a warm bias since around 3,500 (1,400) cases with above normal temperatures were predicted, whereas the observed values were near normal (below normal). On the other hand more than 1,250 cases of above normal temperatures were predicted correctly, as well as about 600 cases of near normal conditions and over 400 cases of below normal conditions. Altogether the categorical forecast ensemble performs quite well with GSS = 0.60. The best performing model in terms of the RV-value is for August 2003 with RV = 77.64%. The ensemble correlation coefficient between forecast and observation is 0.468, and the ensemble mean bias amounts to 0.4°C.

6.2 December temperature in the western and central parts of Mediterranean North Africa

This region includes the Mediterranean areas of Morocco, Algeria, Tunisia, parts of Libya, and the southern Iberian Peninsula. For December, temperature in this region three SST-regimes are relevant. The first relationship describes a connection between western and central North African temperatures and the Pacific Ocean Regime IV (left side of Fig. 8b) with highest cross-correlation coefficients of slightly above 0.4 at a 9 month time lag (right side of

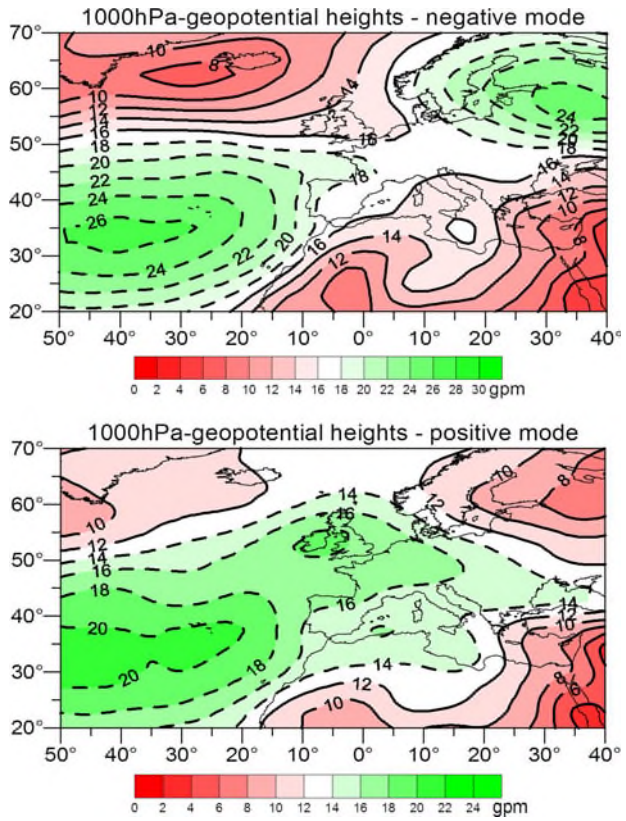

Fig. 7 Composites of the 1,000 hPa-geopotential heights in the forecast month of August, calculated from those cases when the Atlantic Ocean Regime III of Fig. 6b is in its positive (negative) mode in March and temperature in the western Mediterranean region (see Fig. 6a) is above (below) normal in the forecast month of August, see *upper* (*lower*) *panel*

Table 6 3 × 3-contingency table of the forecast ensemble (18 ensemble members) of temperature in August in the western Mediterranean region (489 grid boxes, location of the region see Fig. 6a)

FGSS:0.60	Observation		
	Below normal	Near normal	Above normal
Forecast			
Below normal	432	396	378
Near normal	216	594	432
Above normal	1,404	3,690	1,260

The threshold values for the temperature classes are the limits of the confidence interval for the long- term mean at the 10% significance level (using Student's *t* distribution)

GSS Gerrity skill score

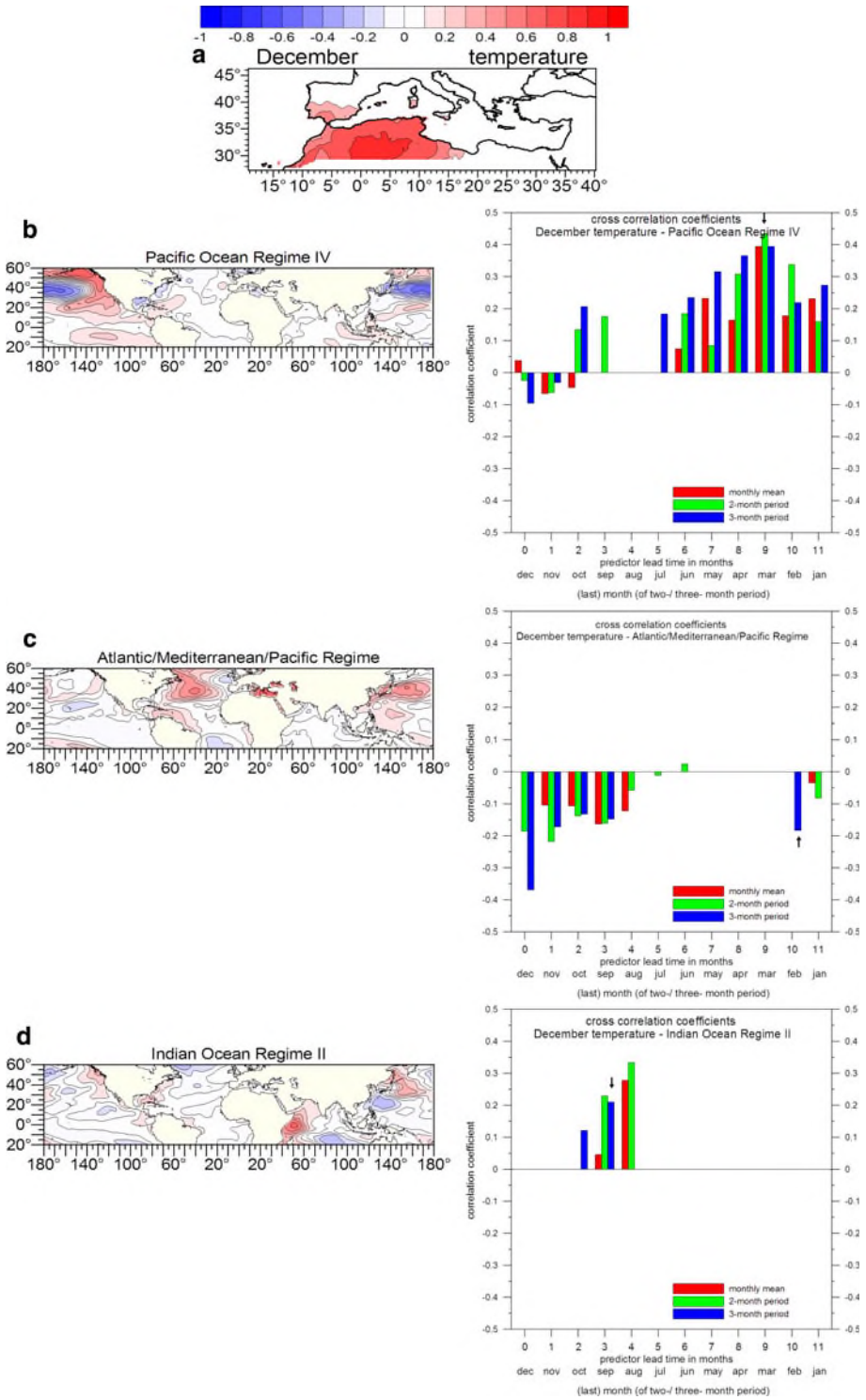

Fig. 8 Relationships of SST-Regimes and Mediterranean temperature. **a** Location of the analysed region (Mediterranean areas of Morocco, Algeria, Tunisia, parts of Libya, and the southern Iberian Peninsula, area marked with *red* colour). **b–d** *Left side* Prototypical loading patterns of the SST-regimes which are selected as predictors for temperature in December in the western and central parts of Mediterranean North Africa. **b–d** *Right side* Corresponding cross-correlation coefficients of the SST-regime scores and regional temperature. The *arrows* indicate which time series of the regimes are selected in the multiple regression equations

Fig. 8b). The regime characteristic of February/March is also selected in the regression models. The Pacific Ocean Regime IV which resembles the Pacific Decadal Oscillation, does not exist or is only realised in an unstable way in late summer and autumn explaining the absence of cross-correlation coefficients during these months in Fig. 8b. The next SST-regime which is selected as predictor for North African December temperatures shows centres of variation in different ocean basins: the eastern Mediterranean Sea, the central North Atlantic and the western North Pacific (left side of Fig. 8c). High SSTs during winter in the above-mentioned oceanic regions are connected to below average temperatures in western and central North Africa during the next winter, 10 months later (right side of

Fig. 8c). Finally, the Indian Ocean Regime II with its centre of variation in the western tropical region, being only present in northern hemispheric summer from July to September, is positively correlated to North African temperatures 2–4 months later (Fig. 8d). This tropical SST-anomaly has a remarkably lower lead time compared to the two extra-tropical SST-regimes which are also selected as predictors for North African December temperature.

The relationship of the Pacific Ocean Regime IV and temperatures of the western part of North Africa in December is further revealed by Table 7 relating the cases with the positive (scores ≥ 0.7) and negative (scores ≤ -0.7) modes of the SST Regime in February/March to below normal, near normal and above normal December temperatures. It can be seen that (averaged over all grid boxes of the region) in 6.5 out of 13 cases of the negative SST-mode in the 1950–2003 period below normal temperatures subsequently occur, and in 8.7 out of 14 cases of the positive SST-mode above normal temperatures have been observed.

The geopotential height composites (1,000 hPa level) of the same cases as in Table 7 reveal that below normal temperatures are connected to a high-pressure system with its centre above the eastern North Atlantic Ocean and Western Europe (upper part of Fig. 9). In front of the anticyclone relatively cold air from northerly directions is advected to the western and central North African region. In contrast to that, the lower part of Fig. 9 indicates that above normal temperatures are associated with an eastward extended subtropical high over the target area. Thus, the late winter SST-pattern, essentially resembling the warm phase of the PDO, promotes a geopotential height pattern in the next winter which causes above normal temperatures in the western and central North African region. In the reverse case, the cool phase of the PDO favours a meridional circulation pattern in the next winter which is connected to below normal temperatures in the western North African region.

Table 7 Cases of positive (scores ≥ 0.7) and negative (scores ≤ -0.7) modes of the Pacific Ocean regime of Fig. 8b in February/March with respect to below normal, near normal and above normal temperature in the western and central North African region (see Fig. 8a) in the subsequent month of December

	Negative mode SST-regime	Positive mode SST- regime
Below normal temperature	6.5	3.4
Near normal temperature	1.6	1.9
Above normal temperature	4.9	8.7
Sum	13	14

The threshold values for the temperature classes are the limits of the confidence interval for the long- term mean at the 10% significance level (using Student's *t* distribution)

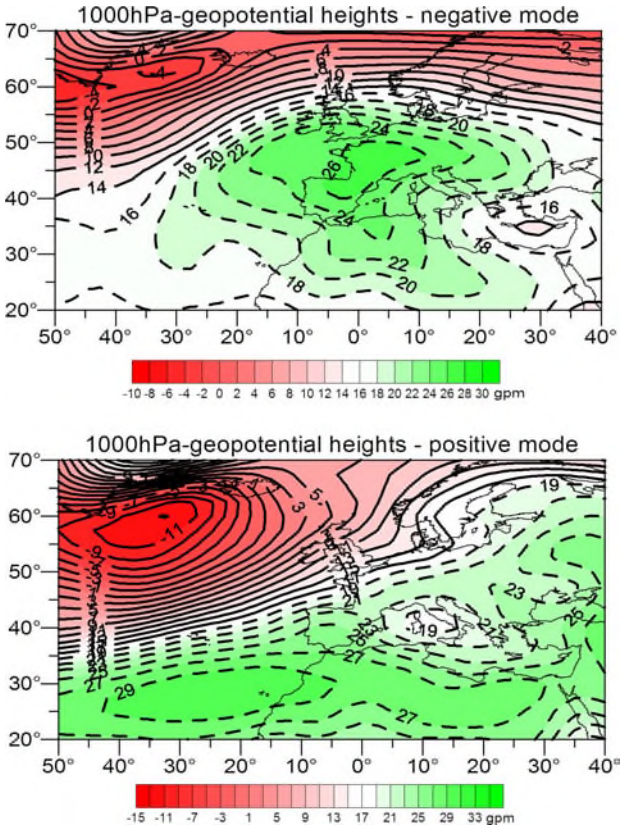

Fig. 9 Composites of the 1,000 hPa-geopotential heights in the forecast month of December, calculated from those cases when the Pacific Ocean Regime IV of Fig. 8b is in its positive (negative) mode in February/March and temperature in the western and central parts of Mediterranean North Africa (see Fig. 8a) is above (below) normal in the forecast month of December, see *upper* (*lower*) *panel*

According to Table 8 summarizing the results of the categorical forecast ensemble, 612 grid box predictions of above normal temperatures also occur in the observation, as well as 1,260 cases of below normal temperatures are correctly predicted. However, for almost 10,000 cases the

Table 8 3 × 3-ontingency table of the forecast ensemble (18 ensemble members) of temperature in December in the western and central North African region (835 grid boxes, location of the region see Fig. 8a)

FGSS:0.53	Observation		
	Below normal	Near normal	Above normal
Forecast			
Below normal	1,260	216	0
Near normal	0	1,566	1,494
Above normal	36	9,846	612

The threshold values for the temperature classes are the limits of the confidence interval for the long- term mean at the 10% significance level (using Student's *t* distribution)

GSS Gerrity skill score

forecasts are too warm (above normal temperatures predicted, but only near normal conditions observed). Despite this fact, the categorical forecast ensemble performs quite well with GSS = 0.53. The best performing model in terms of the RV-value is for December 1996 with RV = 53.95%. The ensemble correlation coefficient between forecast and observation is 0.539, and the ensemble mean bias amounts to 0.3°C.

7 Conclusions

Robust connections of SST-regimes and Mediterranean precipitation and, based on them, skilful predictions of the latter by the former ones can only be established for single regions in particular months of the year. In the winter month of December and the summer months of August and September the focus of predictability is on the Iberian Peninsula, whereas in months of the transitional seasons (mainly March and October) forecasts are possible for the northeastern Mediterranean region around the Aegean Sea. Further isolated prediction skill can be found for regions in the southern and southeastern Mediterranean area during winter.

No prediction skill was found in this study for precipitation in the western Mediterranean area in spring, despite the findings of other studies (Mariotti et al. 2002; Rodo et al. 1997) including significant correlations between ENSO and seasonal rainfall. A possible reason for the lack of prediction skill in spring might be the fact that the correlations are not strong enough throughout the time period under consideration, due to non-stationarities (Mariotti et al. 2002) as well as non-linearities (Gualdi et al. 2003; Pozo-Vasquez et al. 2001, see also Sect. 5.2) in the ENSO-rainfall-relationships. Furthermore, Frias et al. (2010) report that they can obtain prediction skill in spring only under the restriction to strong El Niño/La Niña- events. The interference with other dynamical modes like the Pacific Decadal Oscillation and the NAO (Zanchettin et al. 2008; Brönnimann et al. 2007) might also contribute to this lack of predictability.

For Mediterranean temperature successful predictions can be derived almost exclusively for the regions in the western and southern Mediterranean regions. In the summer months of August and September predictability is focused on the western Mediterranean region, in May and December skilful forecasts can be achieved for western and central North Africa. An exception of the regional focus on the western and southern Mediterranean area is the successful temperature forecast for the central-northern Mediterranean region in November. The better predictability of temperature in the western and southern Mediterranean area compared to other Mediterranean regions suggests that the location of the direct influence within the Atlantic sector and in particular the position of the subtropical high pressure system near the Azores plays a decisive role.

Obviously, only some few of the SST-regimes are important for forecasts in the Mediterranean area, for precipitation most notably SST-regimes of the Atlantic domain like the Atlantic Ocean Regime II (corresponding to the North Atlantic Tripole) and the Atlantic Ocean Regime I (reflecting Tropical Atlantic SST variability). But also SST-regimes of the Pacific Ocean (in particular that one linked to ENSO variability) and of the Indian Ocean have to be considered. For Mediterranean temperatures the North Atlantic Ocean exhibits a considerable influence, especially the Atlantic Ocean Regime III which corresponds to the North Atlantic Horseshoe pattern. But also the tropical and subtropical West Pacific Ocean as well as SST-regimes of the North Pacific Ocean point to a connection with regional temperatures in the Mediterranean area.

Skilful predictions for a whole forecast ensemble can only be achieved by categorical forecasts. In the scope of probabilistic forecasts (without categorization) only individual forecasts show a positive skill. Categorization reduces precipitation/temperature to a low number of classes (three in this case), so that the connections between the SST-regimes and Mediterranean climate variables are considered on a lower-scale basis allowing for a better predictability. That way the method shows skill for some regions and for some seasons. To account for the possibility that this skill is just produced by chance, a dynamical analysis of the SST-regime-climate-correlations has been performed. Composites of geopotential height anomalies compiled from positive and negative modes of those SST-regimes which are associated with Mediterranean temperature/precipitation anomalies reveal the dynamical link between SSTs and Mediterranean climate via the large-scale atmospheric circulation.

The geopotential height composites substantiate that in the western and southern Mediterranean area below normal temperatures can be attributed to meridional flow patterns from northerly directions. On the other hand, above normal temperatures are linked to anticyclonic patterns over the corresponding region thus reflecting autochthonous conditions. Regarding precipitation the composites confirm that below normal precipitation can also be attributed to anticyclonic anomalies. The occurrence of such conditions is clearly linked to a particular mode of important SST-regimes during preceding months or seasons. This points to links via the large-scale atmospheric circulation and allows for linear predictions of Mediterranean precipitation and temperature by particular SST-regimes.

However, this is more difficult for above normal precipitation resulting from increased cyclonic influences. These are linked to varying atmospheric circulation patterns depending on different SST-regimes operating in this dynamical context. Together with the weaker coherence between a particular SST mode and above normal precipitation and the varying sub-periods for predictors in the regression models, it hampers the identification of a straightforward connection.

Furthermore, regarding temperature a warm bias in the forecasts can often be seen. This might be due to a non-linear relationship of the SST-regimes and Mediterranean temperature which is not captured by the applied methodology. This bias might also be caused by the occurrence of short-term atmospheric circulation patterns which are not related to specific antecedent SST-conditions. Dampening effects from other components of the climate system like soil moisture feedbacks or the compensatory effects of the large water volume of the Mediterranean Sea might also be responsible for this bias.

All these features point to necessary improvements of statistical model ensembles for the prediction of regional Mediterranean precipitation and temperature:

- An important aspect should be the incorporation of additional predictor variables. Mainly informations regarding soil moisture, vegetation, snow and ice cover will be decisive. However, just these variables suffer from low data quality and availability. It can be assumed that progress with these data sets will lead to a substantial enhancement in prognostic skill concerning both statistical as well as dynamial forecasts.
- The application of non-linear approaches might help to capture parts in the SST-circulation–climate-relationships which cannot be described by the linear techniques used in this study.
- Extended observational periods may also enhance seasonal predictability. For example, Wilks (2008) has shown that improved predictions of North American temperatures by Pacific Ocean SSTs can be achieved in case of using extended records of observational data, despite the fact that older SST-data include more missing values and are less reliable.
- In general, there is still a considerable need for research concerning ocean–atmosphere-climate-couplings. A better understanding of the process chains between remote oceanic anomalies and regional climate will promote the derivation of appropriate forecast models and enhance their prognostic skill.

Acknowledgments Financial support was provided by the DFG (German Research Foundation) under contract JA 831/3-1.

References

Bahrenberg G, Giese E, Nipper J (1999) Statistische Methoden in der Geographie I. Teubner Studienbücher, Stuttgart, p 233

Breusch TS, Pagan AR (1979) A simple test for heteroscedasticity an random coefficient variation. Econometrica 47:1287–1294

Brönnimann S, Xoplaki E, Casty C, Pauling A, Luterbacher J (2007) ENSO influence on Europe during the last centuries. Clim Dyn 28:181–197

Cassou C, Terray L (2001a) Dual influence of Atlantic and Pacific sst anomalies on the North Atlantic/Europe winter climate. Geophys Res Lett 28:3195–3198

Cassou C, Terray L (2001b) Oceanic forcing of the wintertime low-frequency atmospheric variability in the North Atlantic European Sector: a study with the Arpege model. J Clim 14:4266–4291

Colman A, Davey M (1999) Prediction of summer temperature, rainfall and pressure in Europe from preceding winter North Atlantic Ocean temperature. Int J Climatol 19:513–536

Compagnucci RH, Richman MB (2008) Can principal component analysis provide atmospheric circulation or teleconnection patterns? Int J Climatol 28:703–726

Czaja A, Frankignoul C (1999) Influence of the North Atlantic SST on the atmospheric circulation. Geophys Res Lett 26:2969–2972

Díez E, Primo C, García-Moya JA, Gutiérrez JM, Orfila B (2005) Statistical and dynamical downscaling of precipitation over Spain from DEMETER seasonal forecasts. Tellus A 57:409–423

Drévillon M, Terray L, Rogel P, Cassou C (2001) Midlatitude Atlantic SST influence on European winter climate variability in the NCEP–NCAR Reanalysis. Clim Dyn 18:331–344

Fil C, Dubus L (2005) Winter climate regimes over the North Atlantic and European region and in ERA40 Reanalysis and DEMETER seasonal hindcasts. Tellus A Vol 57:290–307

Frias D, Herrera S, Cofino AS, Gutierrez JM (2010) Assessing the skill of precipitation and temperature seasonal forecasts in Spain: windows of opportunity related to ENSO events. J Clim 23:209–220

Frías D, Fernández J, Sáenz J, Rodríguez-Puebla C (2005) Operational predictability of monthly average maximum temperature over the Iberian Peninsula using DEMETER simulations and downscaling. Tellus 57A:448–463

Gerrity JP (1992) A note on Gandin and Murphy's equitable skill score. Mon Weather Rev 120:2707–2712

Gualdi S, Navarra A, Guilyardi E, Delecluse P (2003) The SINTEX coupled GCM. The tropical Indo-Pacific region. Ann Geophys 46:1–26

Hertig E (2004) Niederschlags- und Temperaturabschätzungen für den Mittelmeerraum unter anthropogen verstärktem Treibhauseffekt. PhD thesis published online at http://www.opus-bayern.de/uni-wuerzburg/volltexte/2004/874

Latif M, Anderson D, Barnett T, Cane M, Kleeman R, Leetmaa A, O'Brien J, Rosati A, Schneider E (1998) A review of the predictability and prediction of ENSO. J Geophys Res 103((C7)):14,375–14,393

Mariotti A, Zeng N, Lau KM (2002): Euro- Mediterranean rainfall and ENSO—a seasonally varying relationship. Geophys Res Lett 29. doi:10.1029/2001GL014248

Mason S, Mimmack G (2002) Comparison of some statistical methods of probabilistic forecasting of ENSO. J Clim 15:8–29

Murphy AH, Epstein ES (1989) Skill scores and correlation coefficients in model verification. Mon Weather Rev 117:572–581

New M, Hulme M, Jones P (1901) Representing twentieth century space-time climate variability. II: development of 1901–1996

monthly grids of terrestrial surface climate. J Clim 13:2217–2238

New M, Hulme M, Jones P (1961) Representing twentieth century space-time climate variability. I: development of a 1961–1990 mean monthly terrestrial climatology. J Clim 12:829–856

Oesterle H, Gerstengarbe FW, Werner PC (2003) Homogenisierung und Aktualisierung des Klimadatensatzes der Climate Research Unit der Universitaet of East Anglia, Norwich. Terra Nostra 2003/6, Alfred- Wegener- Stiftung, Berlin:326–329

Palmer TN, Alessandri A, Andersen U, Cantelaube P, Davey M, Délécluse P, Déqué M, Díez E, Doblas-Reyes FJ, Feddersen H, Graham R, Gualdi S, Guérémy J-F, Hagedorn R, Hoshen M, Keenlyside N, Latif M, Lazar A, Maisonnave E, Marletto V, Morse AP, Orfila B, Rogel P, Terres J-M, Thomson MC (2004) Development of a European multi-model ensemble system for seasonal to inter-annual prediction (DEMETER). Bull Amer Meteorol Soc 85:853–872

Pavan V, Marchesi S, Morgillo A, Cacciamani C, Doblas-Reyes FJ (2005) Downscaling of DEMETER winter seasonal hindcasts over Northern Italy. Tellus A 57:424–434

Pozo-Vasquez D, Esteban-Parra MJ, Rodrigo FS, Castro-Diez Y (2001) The association between ENSO and winter atmospheric circulation and temperature in the North Atlantic region. J Clim 14:3408–3420

Pozo-Vasquez D, Gamiz-Fortis SR, Tovar-Pescador J, Esteban-Parra MJ, Castro-Diez Y (2005) El Nino- Southern Oscillation events and associated European winter precipitation anomalies. Int J Climatol 25:17–31

Preisendorfer RW (1988) Principal component analysis in meteorology and oceanography. Developments in atmospheric Science 17, Amsterdam

Richman MB (1986) Rotation of principal components. J Climatol 6:293–335

Rodo X, Baert E, Comin FA (1997) Variations in seasonal rainfall in Southern Europe during the present century: relationships with the North Atlantic Oscillation and the El Nino-Southern Oscillation. Clim Dyn 13:275–284

Rodriguez-Fonseca B, Castro M (2002) On the connection between winter anomalous precipitation in the Iberian Peninsula and North West Africa and the summer subtropical Atlantic sea surface temperature. Geophys Res Lett 29(18):1863. doi: 10.1029/2001GL014421

Rodriguez-Fonseca B, Polo I, Serrano E, Castro M (2006) Evaluation of the North Atlantic SST forcing on the European and Northern African winter climate. Int J Climatol 26:179–191

Rodwell MJ, Rowell DP, Folland CK (1999) Oceanic forcing of the wintertime North Atlantic Oscillation and European climate. Nature 398:320–323

Royston P (1982) Algorithm AS 181: the W test for normality. Appl Stat 31:176–180

van Oldenborgh, GJ (2005) Comments on 'Predictability of winter climate over the North Atlantic European region during ENSO events' by Mathieu P-P, Sutton RT, Dong B, Collins M. J Clim 18, 2770–2772

von Storch H, Zwiers FW (1999) Statistical analysis in climate research. Cambridge University Press, Cambridge, p 484

Wilks DS (2008) Improved statistical seasonal forecasts using extended training data. Int J Climatol 28:1589–1598

World Meteorological Organization (2007) Standardized verification system for long-range forecasts. New Attachment II-8 to the manual on the global data-processing and forecasting system (WMO-No. 485), vol 1

Zanchettin D, Franks SW, Traverso P, Tomasino M (2008) On ENSO impacts on European wintertime rainfalls and their modulation by the NAO and the Pacific multi-decadal variability described through the PDO index. Int J Climatol 28:995–1006